BIOCHEMISTRY
including biophysical chemistry & molecular biology

Article

pubs.acs.org/biochemistry

Cd Hyperfine Interactions in DNA Bases and DNA of Mouse Strains Infected with *Trypanosoma cruzi* Investigated by Perturbed Angular Correlation Spectroscopy and *ab Initio* Calculations

Philippe A. D. Petersen,[†] Andreia S. Silva,[‡] Marcos B. Gonçalves,[†] André L. Lapolli,[‡] Ana Maria C. Ferreira,[§] Artur W. Carbonari,[‡] and Helena M. Petrilli*[,†]

[†]Departamento de Física de Materiais e Mecânica, Instituto de Física, Universidade de São Paulo, CEP 05508-090 São Paulo, SP, Brazil

[‡]Laboratório de Interações Hiperfinas, Instituto de Pesquisas Energéticas e Nucleares, IPEN-CNEN/SP, 05508-000 São Paulo, SP, Brazil

[§]Departamento de Química Fundamental, Instituto de Química, Universidade de São Paulo, CEP 05508-000 São Paulo, SP, Brazil

ABSTRACT: In this work, perturbed angular correlation (PAC) spectroscopy is used to study differences in the nuclear quadrupole interactions of Cd probes in DNA molecules of mice infected with the Y-strain of *Trypanosoma cruzi*. The possibility of investigating the local genetic alterations in DNA, which occur along generations of mice infected with *T. cruzi*, using hyperfine interactions obtained from PAC measurements and density functional theory (DFT) calculations in DNA bases is discussed. A comparison of DFT calculations with PAC measurements could determine the type of Cd coordination in the studied molecules. To the best of our knowledge, this is the first attempt to use DFT calculations and PAC measurements to investigate the local environment of Cd ions bound to DNA bases in mice infected with Chagas disease. The obtained results also allowed the detection of local changes occurring in the DNA molecules of different generations of mice infected with *T. cruzi*, opening the possibility of using this technique as a complementary tool in the characterization of complicated biological systems.

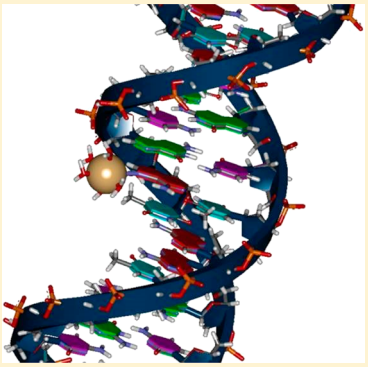

The detection of hyperfine quantities is the goal of many spectroscopic experimental methods, such as Mössbauer spectroscopy, electron paramagnetic resonance (EPR), perturbed angular correlation (PAC), and nuclear magnetic resonance (NMR).[1,2] PAC spectroscopy has some advantages over other hyperfine interactions techniques, being better suited to the study of biomolecules, mainly because it requires an extremely small amount of sample, which allows experiments to be performed under physiological conditions. Further, it can be applied to different physical states, such as samples *in vivo*, samples in solution, frozen samples, etc. Moreover, PAC spectroscopy can also explore the dynamics of biomolecules.[3] PAC spectroscopy provides information about the local electronic structure at the probe nucleus site via the electric hyperfine interaction between the nuclear charge distribution and the electronic surrounding charge distribution, the so-called nuclear quadrupole interaction (NQI). More specifically, in terms of the electric contribution, the electric quadrupole moment Q of the nucleus interacts with the electric field gradient (EFG) at the nuclear site produced by charges outside the nucleus. The EFG is very sensitive to the electric fields arising from charges within the first coordination shell around the probe nuclei.[1] Therefore, via the EFG, PAC spectroscopy can probe an extremely high spatial resolution, within a single atomic bond length. On the other hand, because the EFG is a ground state property, it is also easily calculated as long as the charge density around the probe nucleus is known from first-principles calculations, which can, today, be reliably performed in the framework of the density functional theory (DFT). Because of its high sensitivity, the EFG is a very powerful parameter that can be used in comparisons between experimental and calculated values to investigate local environments. In bioinorganic chemistry, the PAC technique is used to measure the hyperfine interactions at a specific metal probe (e.g., Cd, In, Ta, or Hf) bound to key biomolecules, such as deoxyribonucleic acid (DNA) or proteins, providing structural and dynamic information about the contact site with the probe.[4]

In this work, PAC spectroscopy was used to investigate the hyperfine interactions at Cd probe nuclei bound to free nucleobase (NB) molecules as well as to DNA of different mouse strains infected with *Trypanosoma cruzi*, the protozoan that causes Chagas disease. Differences in the resistance of people to *T. cruzi* indicate that the genetic constitution of the host can significantly influence the development of the disease.[5,6] Further, the analysis of mouse strains infected with *T. cruzi* suggests the importance of the genetic constitution on the survival of the host.[5−7] On the other hand, DFT

Received: December 18, 2013
Revised: April 30, 2014
Published: May 6, 2014

calculations and PAC measurements may be used to provide details about local structural changes in the DNA formed along different generations of mouse strains by monitoring the local structure of the Cd−DNA complexes.

Metal ions can interact with nucleic acids in two distinct modes of binding: diffuse binding and site binding.[8] In diffuse binding, the metal and the nucleic acid retain their hydration layer and the interaction occurs mainly through water molecules.[9] This is a long-range Coulomb interaction in which the positive metal ions accumulate around the DNA in a delocalized form. In site binding, on the other hand, the metal coordinates to specific coordinating atoms in the nucleic acids (Figure 1). This coordination can be direct at the inner sphere,

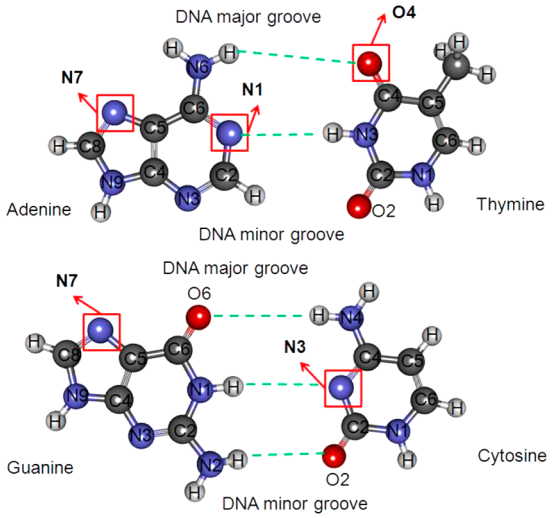

Figure 1. Metal binding sites at the DNA bases (NBs), as suggested by Hadjiliadis and Sletten,[8] are denoted with squares linked to arrows. The green lines denote the hydrogen bonds between base pairs.

after dehydration of both the metal ion and the nucleic acid binding site. Another possible coordination scenario can arise when a metal water hydration layer is kept intact, and the metal ion and the nucleic acid ligands share hydration shells. The likelihood of metal ions binding to the DNA at the minor groove is smaller than the likelihood at the major groove.[8] In the major groove, a large number of metal ions, including Cd^{2+},[10,11] prefers to bind at bases or base pairs of the nucleotides as shown in Figure 1. Cd^{2+} ions have multiple possible DNA binding sites with variable affinities, although they are not very high in comparison to those of other divalent ions. According to the literature,[12] the N7 position of guanine seems to be the strongest intrinsic binding site for these ions. Some reported binding constants of Cd-bound nucleoside species are 1.53 ± 0.07 for guanosine (Guo),[13] 0.91 ± 0.07 for cytidine (Cyd), and 0.64 ± 0.03 for adenosine (Ado).[14]

In this work, the behavior of static and dynamic NQI at Cd sites bound to DNA of different mouse lineages (A/J, C57BL/6, B6AF1, BXA1, and BXA2), infected with the Y-strain of *T. cruzi*, has been investigated. PAC spectroscopy was used to measure the EFG at ^{111}In (^{111}Cd) and ^{111m}Cd (^{111}Cd) nuclei bound to NBs and DNA. To determine the exact location of the probe in the DNA or NBs, we conducted DFT calculations for the NBs. The most probable positions, where Cd ions can bind to NBs, were investigated, and the obtained EFG values were compared to the PAC experimental data. In addition, EFG measurements of Cd in NBs were compared to those in DNA, to investigate the EFG behavior in different generations of mouse strains infected with the Y-strain of *T. cruzi*.

COMPUTATIONAL DETAILS

The Car−Parrinello Projector Augmented Wave (CP-PAW) code[15,16] was used to perform all the reported calculations. CP-PAW employs DFT calculations in the Kohn−Sham (KS) formalism.[17] Generalized gradient approximation (GGA) provided by Perdew, Burke, and Ernzerhorf (PBE) was used for the exchange-correlation functional to make corrections of nonhomogeneous effects of the local density approximation (LDA) with the inclusion of terms of gradient and higher-order derivatives of the density.[18] The PAW formalism is an *ab initio* k-space all-electron method in which the wave function is expanded on an augmented plane wave basis. All systems studied were simulated as isolated molecules using the repeated super cell approach. A distance of 7 Å between periodic images was used to prevent wave function overlap and a charge decoupling scheme to avoid the artificial electrostatic interactions among the other unit cells.[15] The PAW method is very efficient for metal−organic systems and widely used for calculations of systems such as those presented here.[19] Geometry optimizations were performed using 35 Ry as the corresponding cutoff energies in the expansions of the wave functions and 4 × 35 Ry charge densities.

The structure of the NB was obtained considering the canonical form and the initial atomic positions from the single-crystal X-ray diffraction data.[8,20,21] Further, the Cd ion was included in sites of NBs as proposed in the literature[8] as shown in Figure 1. To complete the ion coordination sphere and because one of the measurements was performed in aqueous solution, three, four, and five water molecules were inserted explicitly in the studied systems. The Cd ion has six coordination sites available in an octahedral structure when it is bound to NB ligands.[22−24] Nevertheless, other coordination types were also considered and performed as starting geometries. All systems studied here were calculated considering the steady oxidation state of Cd^{2+}; i.e., the total charge of the system was set to +2e.

Cd bound to the N1 adenine site was not simulated because the N1 site is usually located in the DNA minor groove and is hydrogen bonded to the thymine. Thus, because of steric hindrance, the interaction of Cd with water molecules at the N1 site of adenine is more unlikely to occur. The EFG is also implemented on the CP-PAW code, and further information can be found elsewhere.[25]

EXPERIMENTAL METHODOLOGY

DNA molecules were obtained from mouse strains A/J, C57BL/6, B6AF1, BXA1, and BXA2 from the Multidisciplinary Center for Biological Research (CEMIB) at University of Campinas, Brazil, where mice are maintained free from pathogenic agents (SPF). A/J and C57BL/6 strains are original parent strains and are known to differ in susceptibility to more than 30 traits.[26] In particular, A/J and C57BL/6 inbred strains of mice when they were inoculated with the Y-strain of *T. cruzi* behaved as susceptible and relatively resistant, respectively, with respect to parasitemia when mortality was analyzed.[27] Hybrid B6AF1 mice are offspring of a cross between C57BL/6 females and A/J males and show relative resistance to *T. cruzi* infection like that of the C57BL/6 parent strain. BXA strains, the 20th generation of brother−sister inbreeding, were constructed

dx.doi.org/10.1021/bi401680h | *Biochemistry* 2014, 53, 3446−3456

using reciprocal crosses between C57BL/6 (B) and A/J (A) strains as progenitors. Mice from the BXA1 strain show the same immune response to *T. cruzi* infection as those from the C57BL/6 strain, while mice from the BXA2 strain are considered to be susceptible to this infection; however, they remain alive for a longer time than mice from the A/J strain.

Nucleobases, adenine ($C_5H_5N_5$), cytosine ($C_4H_5N_3O$), thymine ($C_5H_6N_2O_2$) (all ≥99% pure), and guanine ($C_5H_5N_5O$) (98% pure), used in this work were commercially purchased from Sigma-Aldrich and used as received. In PAC measurements, a small amount (0.1 mol) of each DNA base was dissolved in 100 mL of deionized water or buffer solution, up to a concentration of 1×10^{-6} mol/μL, and stored at room temperature until each sample was used. DNA samples of different mouse lineages infected with the Y-strain of *T. cruzi* used in this work were extracted from mouse tails and ear punches and stored at 4 °C until the samples were used. DNA samples as well as samples of DNA bases were directly marked by coordinating to ^{111}In from $^{111}InCl_3$ or ^{111m}Cd from $^{111m}Cd(NO_3)_2$ solutions. The carrier free $^{111}InCl_3$ solution was purchased from MS Nordion, Canada. The $^{111m}Cd(NO_3)_2$ solution was obtained by the irradiation of 5 mg of Cd metal in the IEA-R1 research reactor at IPEN for 2 h, in a thermal neutron flux of ∼5×10^{13} N cm^{-2} s^{-1}. After irradiation, the Cd metal was dissolved in 0.3 mL of 1 M nitric acid, which was completely evaporated. The resulting salt was then dissolved in 0.5 mL of deionized water, resulting in a $Cd(NO_3)_2$ concentration of 1×10^{-7} mol/μL containing the ^{111m}Cd probe nuclei. Samples of an aqueous solution of DNA or NBs with radioactive ^{111}In were prepared from an aliquot of 50 μL of a solution of $^{111}InCl_3$ containing ∼10 μCi of the radioactive ^{111}In, so that the In:biomolecule concentration ratio was 1:infinity (1:∞). Samples of aqueous solutions of NBs with ^{111m}Cd were prepared by mixing an aliquot of 50 μL of NB stock solutions with 5 μL of a $Cd(NO_3)_2$ solution containing the ^{111m}Cd probe nuclei, resulting in a Cd:NB molecule concentration ratio of 1:100. Samples of NBs in buffer solution (0.01 M) were prepared by dissolving 0.1 mol of NB in 100 mL of a phosphate buffer solution (pH ∼7.0). An aliquot of 50 μL of this solution was mixed with 5 μL of a $Cd(NO_3)_2$ solution containing the ^{111m}Cd probe nuclei, resulting in a Cd:NB molecule concentration ratio of 1:100. Samples of NBs in the solid state were prepared by adding ∼1 μL of the solution containing the probe nuclei to 0.01 M NB solution, which was subsequently dried under infrared light. Aqueous solutions of probe nuclei were prepared simply by adding ∼1 μL of a $^{111}InCl_3$ solution or ∼5 μL of a $^{111m}Cd(NO_3)_2$ solution to 50 μL of deionized water. ^{111m}Cd (^{111}Cd) probe nuclei in a buffer solution was prepared by adding ∼5 μL of a $^{111m}Cd(NO_3)_2$ solution to 50 μL of a buffer solution. The concentration of the ^{111}In (^{111}Cd) probe in these samples is much lower than the concentration of DNA or NBs in the final solution, so that an infinite dilution was considered.[28]

PAC measurements were taken in a spectrometer with four BaF_2 detectors that generate 12 coincidence spectra $W(\theta,t)$. These spectra were analyzed by TDPAC software, which yields the spin rotation $R(t)$ curve, given by the combination of the coincidence functions $W(\theta,t)$:

$$R(t) = A_{22}G_{22}(t) = \frac{\overline{W(180°, t)} - \overline{W(90°, t)}}{\overline{W(180°, t)} - 2\overline{W(90°, t)}} \quad (1)$$

where

$$\overline{W(180°, t)} = \sqrt[4]{\prod_{i=4}^{4} C_i(180°, t)} \quad (2)$$

and

$$\overline{W(90°, t)} = \sqrt[8]{\prod_{i=8}^{8} C_i(90°, t)}$$

$C_i(\theta,t)$ terms are the coincidence spectra for all different combinations of two detectors at angles (θ) of 90° and 180° after subtraction of the effects of unwanted accidental coincidences $C_A(t)$: $C_i(\theta,t) = C_i(\theta,t) - C_A(t)$. From the $R(t)$ curve, it is possible to obtain ω_n, the transition frequencies corresponding to the splitting of the intermediate energy level in the γ cascade of the probe nucleus due to the presence of an electric field gradient that originated from the electronic neighborhood.[29,30] In the case of static electric quadrupole hyperfine interaction, the perturbation factor $G^i_{22}(t)$, which contains detailed information about the interaction, can be written as

$$G_{22}(t) = S_{20} + \sum_{n=1}^{3} S_{2n} \cos(\omega_n t) \exp(-\omega_n{}^2\tau_R{}^2/2) \times \exp(-\omega_n{}^2\delta^2t^2/2) \quad (3)$$

where amplitudes S_{2n} and frequencies ω_n depend on the nuclear quadrupole frequency $\omega_Q = (eQV_{zz})/4I(2I - 1)\hbar$, where e is the electron charge, Q is the electric quadrupole moment of the probe nucleus, which for the 245 keV sate of ^{111}Cd is 0.83(13) b,[31] $\hbar$ is Planck's constant, and I is the nuclear spin quantum number. The EFG is a traceless symmetric tensor with components denoted V_{ij}, defined by the second derivative of the Coulomb potential $V(\mathbf{r})$ at the nuclear site. The EFG tensor is traceless ($V_{xx} + V_{yy} + V_{zz} = 0$) in the principal axis system, V_{xx}, V_{yy}, and V_{zz} being the diagonal elements. The usual choice is to define $|V_{xx}| \leq |V_{yy}| < |V_{zz}|$; hence, V_{zz} is the largest eigenvalue of the EFG tensor. Instead of specifying three of the diagonal elements, usually V_{zz} and the asymmetry parameter $\eta = |(V_{xx} - V_{yy})/V_{zz}|$ are reported; the largest component of the EFG tensor, V_{zz}, is usually termed the EFG. The terms $\exp(-\omega_n{}^2\tau_R{}^2/2)$ and $\exp(-\omega_n{}^2\delta^2t^2/2)$ account for effects of the finite time resolution τ_R of the detectors and the distribution of the quadrupolar frequency around a mean value with a width δ, respectively. The measured perturbation function of polycrystalline samples is modeled by

$$R(t) = A_{22}G_{22}(t) = A_{22}\sum_i f_i G^i{}_{22}(t) \quad (4)$$

where A_{22} is the unperturbed angular correlation coefficient and f_i values are the fractional site populations that take into account the fact that the probe nuclei can occupy different sites in the samples with a corresponding $G^i_{22}(t)$.

If the electric quadrupole frequency (ν_Q) is known, the V_{zz} value can be obtained from the equation

$$\nu_Q = \frac{eQV_{zz}}{h} \quad (5)$$

PAC measurements of DNA and NB samples in solution were taken at room temperature (295 K) and at the liquid nitrogen temperature (77 K) in a conventional fast-slow coincidence setup with four conical BaF_2 detectors. A detailed description of experimental method can be found elsewhere.[32]

At 295 K, the solution was liquid and, therefore, the presence of the rotational diffusion effect is expected. This effect is characterized by the rotational correlation time τ_C, which describes changes in the spin orientation of the probe nucleus due to a random change in its environment. The larger the τ_C, the slower the molecular motion. In the case of fast reorientation, the perturbation function becomes[33]

$$G_{22}(t) = e^{-\lambda_2 t} \quad (6)$$

where λ_2 is a typical relaxation constant that is proportional to the square of the spin-independent quadrupole frequency ν_Q and τ_C. For the spin of the intermediate level of the g-cascade $I = {}^5/_2$, which is the case for both probe nuclei used in this work, the relaxation constant is[4,28]

$$\lambda_2 = 2.49\nu_Q{}^2(1 + \eta^2/3)\tau_C \quad (7)$$

The influence of the dynamic interaction is stronger when $\nu_Q\tau_C \approx 1$, and as a consequence, the effect on the PAC spectrum is a fast damping of the anisotropy. There are two other possible situations. (1) When the quadrupole interaction fluctuation is fast ($\nu_Q\tau_C \ll 1$), because the fluctuation time is small compared with the time scale of the quadrupole interaction characterized by ν_Q, the nucleus loses the phase coherence and the perturbation function becomes an exponential decay as described by eq 6. (2) When the quadrupole interaction fluctuation is slow ($\nu_Q\tau_C \gg 1$), the fluctuation time here is long, compared with the time scale of the quadrupole interaction, and the effect is a slow damping of the anisotropy. In the limit where $\tau_C \to \infty$, the interaction is purely static. Only in this case is it possible to determine simultaneously the quadrupole frequency ν_Q and the asymmetry parameter η, as well as the hyperfine parameters related to the local structure around the probe nucleus in the biomolecule.[33] Such a situation is expected for the measurements at 77 K, when the solution is frozen.

RESULTS AND DISCUSSION

Experimental Results. PAC spectra measured with ^{111}In (^{111}Cd)/DNA samples at 77 K were fit with a model given by eqs 3 and 4 for static interactions, considering two fraction sites. The major fraction was characterized by abundances $f \sim 55\%$ with a ν_Q of ~135 MHz, for A/J, C57BL/6, and B6AF1 samples, and $f \sim 65\%$ with a ν_Q of ~200 MHz, for BXA1 and BXA2 samples. The hyperfine parameters for the major fractions produced by the fits are listed in Table 1. All frequencies were found to be broadly distributed ($\delta \sim 40\%$) as shown in Figure 2, which shows spectra for all samples, measured at 77 K. The minor fraction was also characterized by broadly distributed frequencies with higher values (in the ~270 MHz to ~350 MHz range). Frequencies for both minor and major fractions are quite different from the quadrupole frequency ν_Q = 86(3) MHz (δ = 20%), obtained when the ^{111}In (^{111}Cd) probe in aqueous solution ($^{111}InCl_3$ dissolved in deionized water) was used. Therefore, we concluded that

Table 1. Hyperfine Parameters Measured at 77 K with PAC Spectroscopy Using ^{111}In (^{111}Cd) as Probe Nuclei and the Corresponding EFGs (V_{zz})

	ν_Q (MHz)	η	V_{zz} ($\times 10^{21}$ V/m^2)
nucleobase			
adenine	142 ± 7	0.6 ± 0.1	7.1 ± 0.7
adenine powder	140 ± 9	0.4 ± 0.1	7.0 ± 0.8
cytosine	148 ± 8	0.6 ± 0.1	7.4 ± 0.8
guanine	155 ± 9	0.4 ± 0.1	7.7 ± 0.8
thymine	145 ± 9	0.7 ± 0.1	7.2 ± 0.8
DNA strain			
A/J	136 ± 9	0.6 ± 0.1	6.8 ± 0.7
C57BL/6	133 ± 7	0.2 ± 0.1	6.6 ± 0.6
B6AF1	130 ± 9	0.5 ± 0.1	6.5 ± 0.8
BXA1	222 ± 8	0	11.1 ± 0.8
BXA2	196 ± 7	0	9.8 ± 0.6
aqueous solution	86 ± 4	0.6 ± 0.1	4.3 ± 0.4

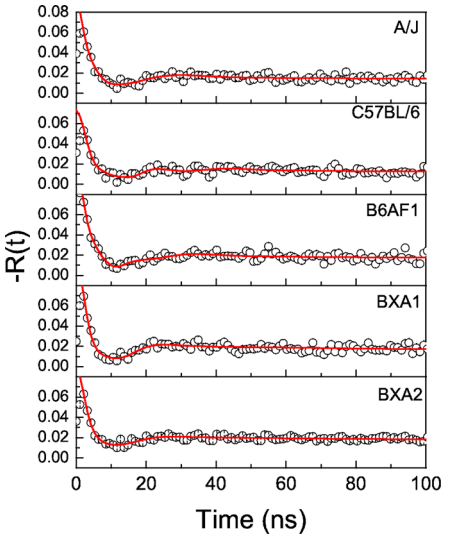

Figure 2. PAC spectra of DNA samples of different mouse lineages measured with ^{111}In (^{111}Cd) probes at 77 K.

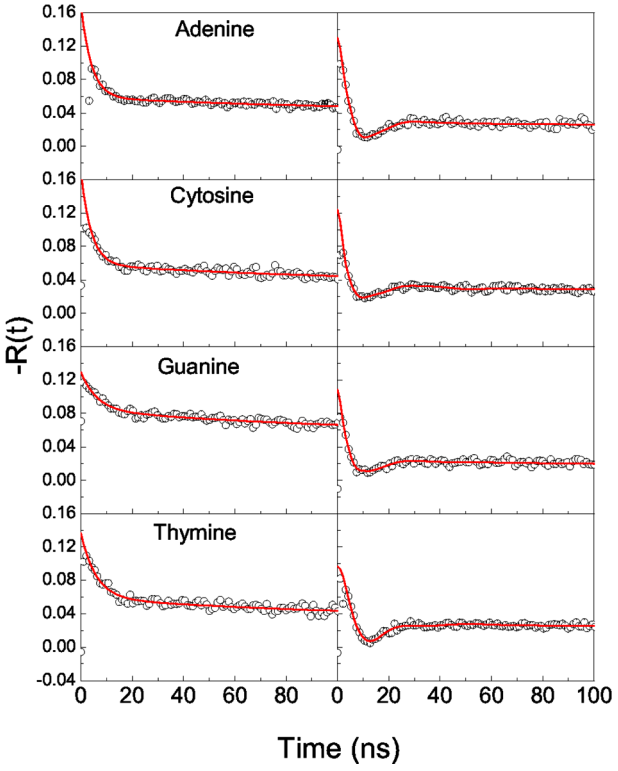

Figure 3. PAC spectra of the nucleobases measured with ^{111}In (^{111}Cd) probes at room temperature (left) and 77 K (right).

dx.doi.org/10.1021/bi401680h | Biochemistry 2014, 53, 3446−3456

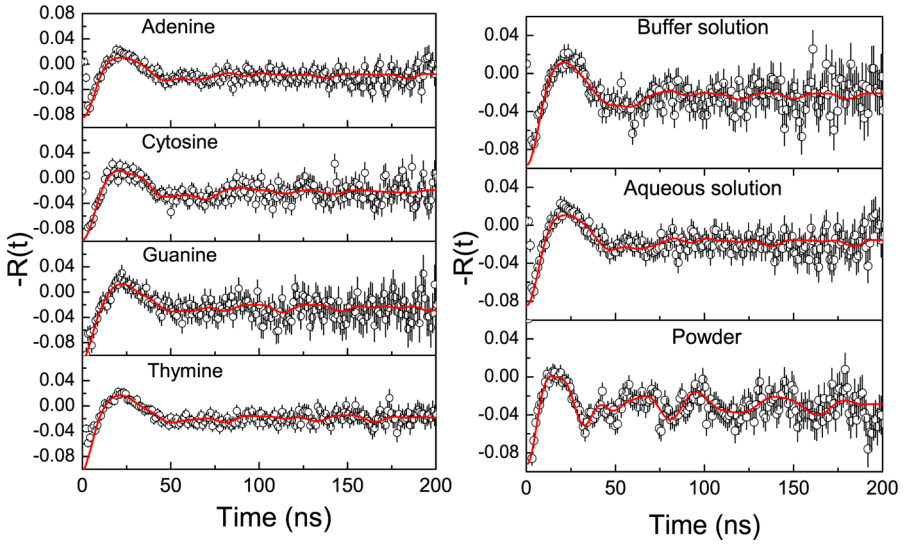

Figure 4. PAC spectra measured with ^{111m}Cd (^{111}Cd) probes at 77 K for indicated nitrogenous bases in aqueous solution (left). Spectra for adenine samples in a buffer solution, in an aqueous solution (same as left panel), and as a powder are also shown in the right panel.

Table 2. Hyperfine Parameters for Nitrogenous Bases in Aqueous Solutions (AS), in Buffer Solutions (BS), and as Powder Samples (PW) Measured at 77 K via PAC Spectroscopy Using ^{111m}Cd (^{111}Cd) as Probe Nuclei and the Corresponding EFGs (V_{zz})

nucleobase	ν_{Q_1} (MHz)	η_1	V_{zz_1} ($\times 10^{21}$ V/m^2)	ν_{Q_2} (MHz)	η_2	V_{zz_2} ($\times 10^{21}$ V/m^2)
adenine AS	87 ± 4	0.49 ± 0.05	4.3 ± 0.2	145 ± 3	0.10 ± 0.06	7.2 ± 0.5
adenine BS	85 ± 4	0.61 ± 0.05	4.2 ± 0.2	126 ± 3	0.95 ± 0.06	6.3 ± 0.5
adenine PW	–	–	–	131 ± 2	0.51 ± 0.04	6.5 ± 0.4
cytosine AS	81 ± 3	0.58 ± 0.05	4.1 ± 0.1	147 ± 2	0.17 ± 0.06	7.3 ± 0.4
cytosine BS	81 ± 4	0.55 ± 0.05	4.1 ± 0.2	149 ± 3	0.51 ± 0.05	7.4 ± 0.5
cytosine PW	–	–	–	120 ± 2	1	6.0 ± 0.6
guanine AS	90 ± 5	0.48 ± 0.06	4.5 ± 0.3	125 ± 2	0.33 ± 0.04	6.2 ± 0.5
guanine BS	83 ± 4	0.53 ± 0.07	4.1 ± 0.2	124 ± 3	0.67 ± 0.05	6.2 ± 0.5
guanine PW	–	–	–	118 ± 2	0.34 ± 0.03	5.9 ± 0.6
thymine AS	79 ± 5	0.53 ± 0.06	4.0 ± 0.4	126 ± 3	0.49 ± 0.03	6.3 ± 0.5
thymine BS	83 ± 4	0.60 ± 0.05	4.1 ± 0.2	132 ± 3	0.84 ± 0.04	6.6 ± 0.4
thymine PW	–	–	–	123 ± 4	0.73 ± 0.05	6.1 ± 0.6
aqueous solution	85 ± 4	0.54 ± 0.05	4.3 ± 0.2	–	–	–
buffer solution	87 ± 5	0.54 ± 0.05	4.3 ± 0.2	–	–	–

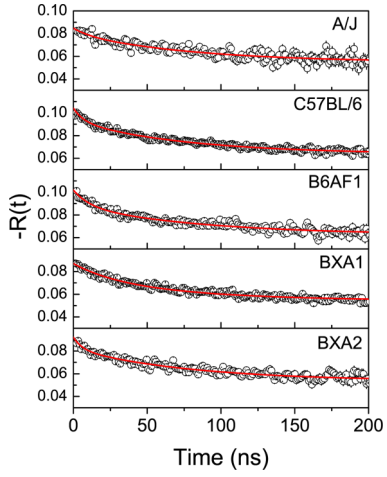

Figure 5. PAC spectra of DNA samples measured with ^{111}In (^{111}Cd) probes at 295 K.

Table 3. Relaxation Constants Extracted from the Fits to Experimental Data Measured with ^{111}In (^{111}Cd) at 295 K[a]

	$\lambda_{2(1)}$ (MHz)	τ_C ($\times 10^{-11}$ s)	$\lambda_{2(2)}$ (MHz)
nucleobase			
adenine	7.4 ± 1.3	13.3 ± 2.5	248 ± 16
cytosine	9.1 ± 1.8	15.1 ± 2.4	253 ± 29
guanine	10.0 ± 1.6	15.9 ± 2.5	163 ± 21
thymine	8.7 ± 2.0	14.6 ± 2.6	172 ± 15
DNA strain			
A/J	12.2 ± 1.9	23.7 ± 4.1	98 ± 18
C57BL/6	13.0 ± 0.9	29.1 ± 3.5	141 ± 26
B6AF1	11.4 ± 1.3	25.1 ± 4.0	93 ± 24
BXA1	11.8 ± 1.9	9.6 ± 2.7	63 ± 21
BXA2	12.4 ± 1.0	13.0 ± 2.5	166 ± 31
aqueous solution	0.15 ± 0.01	0.73 ± 0.20	–

[a]Also shown, the calculated rotational correlation time (τ_C).

almost all probe nuclei are bound to DNA molecules and very little, if any, probe nuclei are bound to only water molecules.

dx.doi.org/10.1021/bi401680h | *Biochemistry* 2014, 53, 3446−3456

Table 4. Adenine, Thymine, Cytosine, and Guanine EFG (V_{zz}) Results with ^{111}In (^{111}Cd) as Probe Nuclei and the Corresponding Cd Coordination

	Cd coordination	V_{zz} ($\times 10^{21}$ V/m^2) (CP-PAW)
nucleobase		
adenine	$5(N_2O_3^{water})$	9.6
	$6(NO_5^{water})$	7.4
cytosine	$6(NO_5^{water})$	5.2
	$6[NO]O_4^{water}$ (binding to O_2)	8.3
guanine	$4(NO_3^{water})$	11.7
	$6(NO_5^{water})$	4.8
	$6[NO]O_4^{water}$	5.8
thymine	$6(OO_5^{water})$	7.1
base pair		
guanine and cytosine	$6[NO]^{guanine}O_4^{water}$	7.6
	$6[N]^{guanine}O_5^{water}$	8.4
adenine and thymine	$6[N]^{adenine}O_5^{water}$	7.2

To investigate the positions at the DNA molecules to which ^{111}In (^{111}Cd) probes are bound, we conducted analogous PAC measurements on adenine, thymine, guanine, and cytosine, the DNA nitrogenous bases, at 77 and 295 K, and compared the results with those obtained from DFT calculations. PAC measurements with ^{111}In (^{111}Cd) at 77 K showed a major fraction site occupation for all NB samples with abundances $f >$ 90% and ν_Q values within the range of 140−155 MHz, which was assigned to ^{111}Cd probes bound to NB molecules. Results for this fraction are listed in Table 1, where the corresponding principal component of the EFG tensor (V_{zz}) is also displayed. The Q value of 830 ± 13 mb for Cd was used to obtain the V_{zz} measurements.[31,34] Because the observed frequency distribution for all samples is wide ($\delta \sim 40\%$), one can consider that the frequencies and asymmetry parameters as well as the corresponding V_{zz} obtained for all NBs are practically equal. The minor fractions with small abundances are probably due to probe nuclei bound to water molecules. PAC spectra for all nucleobases at 295 and 77 K are shown in Figure 3.

The broad δ values observed at 77 K can be in part due to the after-effects, which are caused by the electron capture process when ^{111}In decays to ^{111}Cd. More details about how the after-effect can disturb the PAC measurements in biomolecules can be found elsewhere.[28] The after-effect, therefore, results in a dynamic process that, for the static interaction at 77 K, can contribute to the decrease in the amplitude of the PAC spectra over time. As a consequence, an additional contribution to the frequency distribution makes the uncertainty in the quadrupole values large. To eliminate the influence of the after-effects in the quadrupole frequency measurements, we have used ^{111m}Cd (^{111}Cd) probes to measure ν_Q at 77 K in NB samples. Because ^{111m}Cd is formed at one of the excited states of ^{111}Cd, which decays to the ground state via the 245 keV intermediate state, this probe does not produce after-effects during PAC measurements and the uncertainty in the measured quadrupole frequency tends to be smaller than that for ^{111}In (^{111}Cd) probes. Consequently, we conducted PAC measurements at 77 K using ^{111m}Cd (^{111}Cd) probes in NBs in aqueous solution, in buffer solution at pH 7, and in powder samples. The resulting spectra for all NBs in aqueous solutions are shown in the left part of Figure 4, which also shows, in the right part, the corresponding spectra for adenine in a buffer solution and as a powder sample.

The PAC spectra for NB samples measured with ^{111m}Cd (^{111}Cd) at 77 K were fit with two fraction sites. The results for the observed hyperfine parameters obtained from the fit to experimental spectra are listed in Table 2 along with the corresponding V_{zz} values. For NBs in aqueous solution or in buffer solution, the major fraction ($f \sim 85\%$) was characterized by ν_Q values in the range from ∼80 to ∼90 MHz and a frequency distribution $\delta \sim 20\%$. The minor fraction observed for these samples was characterized by well-defined ($\delta < 5\%$) frequencies in the range from ∼125 to ∼150 MHz. Results for PAC measurements in NB powder samples of adenine indicated almost a single fraction ($f > 95\%$) with a well-defined ν_Q of 131(2) MHz and an η of 0.51(2), as shown in Figure 4. Results for the other NB powder samples show a significant fraction ($f \sim 30\%$) with a ν_Q of ∼120 MHz, but for a large fraction, an unperturbed ($\nu_Q \sim 0$) function was observed, which means that the major fraction of probe nuclei did not bind to the NB molecules. This observation can be explained by the supposition that the binding of Cd ions to NB molecules is probably more efficient when it is mediated by water.

In Table 2, values of V_{zz} for all NBs in aqueous solution or buffer solution are around 4×10^{21} V/m^2 for the fraction with a higher abundance, which was assigned to probe nuclei bound to water molecules, because measurements with ^{111m}Cd (^{111}Cd) in water and in buffer solution produce the same V_{zz}. This site fraction occupation is quite different from that observed for measurements with ^{111}In (^{111}Cd), which is explained by the concentration of Cd (including the radioactive ^{111m}Cd) being much higher than the concentration of radioactive ^{111}In used in the solutions. Consequently, the probability that ^{111m}Cd nuclei bind to water molecules is higher than that for ^{111}In. V_{zz} values for the fraction of probe nuclei bound to NB molecules are all in the range from $\sim 6 \times 10^{21}$ to $\sim 7 \times 10^{21}$ V/m^2, which indicates that the local environment of the probe nuclei bound to each NB molecule is practically the same. The lowest values were obtained for powder samples of NBs, indicating that water molecules have some influence on the measured V_{zz} for NBs in aqueous solutions.

Considering the frequency distribution and the experimental uncertainty in the V_{zz} values for all NBs in aqueous solution measured with both ^{111}In (^{111}Cd) and ^{111m}Cd (^{111}Cd) probe nuclei, listed in Tables 1 and 2, respectively, we can infer that the V_{zz} is almost the same for both probes.

The dynamic behavior of DNA and NB molecules were monitored experimentally by the determination of the relaxation constant λ_2 by PAC measurements of the aqueous solutions at 295 K. Using eq 7 with the measured ν_Q and λ_2, it was possible to calculate the rotational correlation time τ_C, used to characterize the dynamic behavior of the studied molecule. PAC spectra for the DNA samples measured with the ^{111}In (^{111}Cd) probe at 295 K are shown in Figure 5.

As one can easily observe in the PAC spectra for DNA samples at 295 K, the model given by eq 6 will not fit to the experimental data because of a non-zero baseline at times after ∼200 ns, which correspond to an unperturbed fraction due to unbound probe atoms or some light molecules containing the probe atoms. Therefore, experimental data obtained with the ^{111}In (^{111}Cd) probe at 295 K could only be appropriately modeled by the following function, in which two relaxation constants and a parameter a_0, which takes into account the unperturbed fraction, are considered:[28]

dx.doi.org/10.1021/bi401680h | Biochemistry 2014, 53, 3446−3456

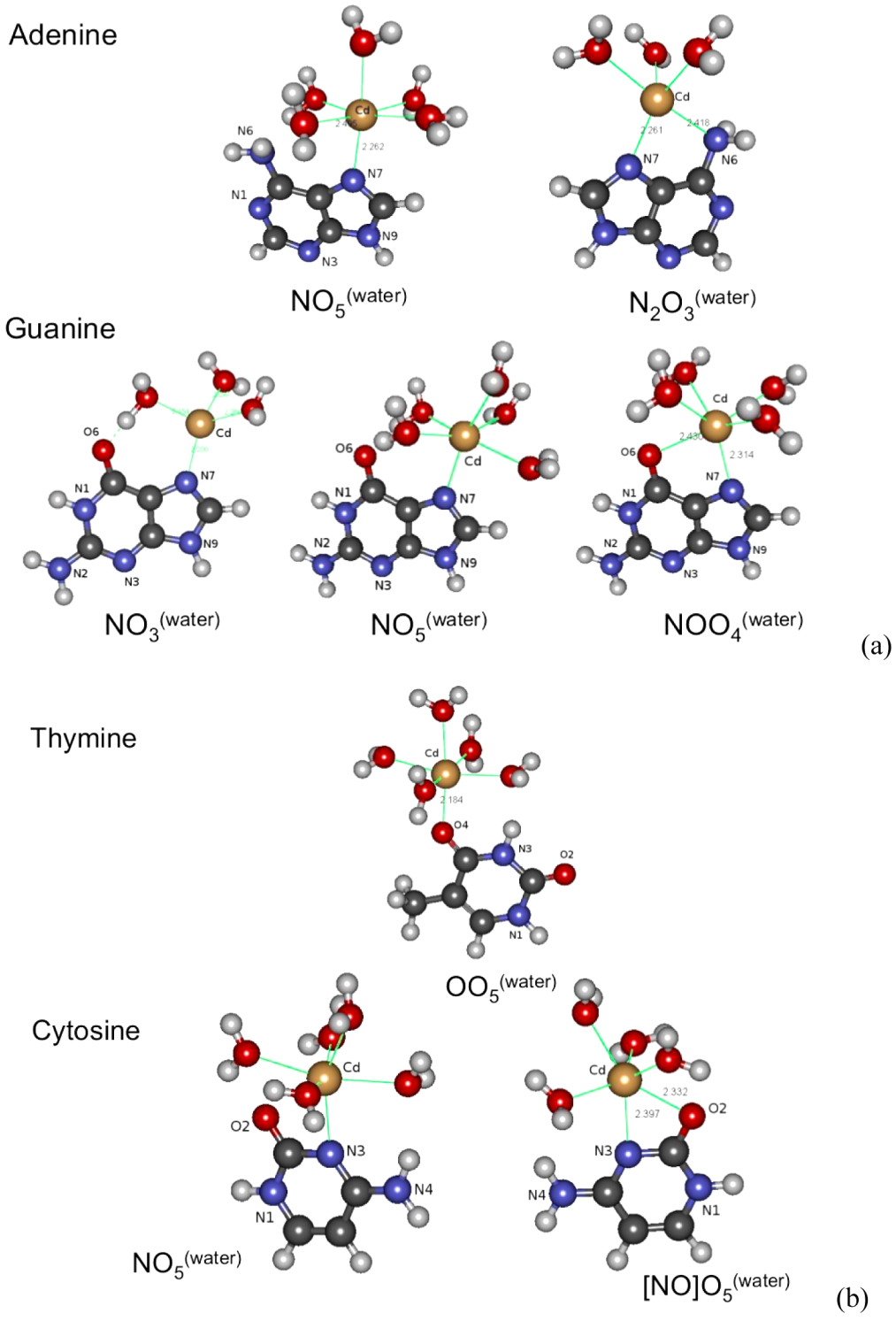

Figure 6. Geometry optimizations and Cd coordination in (a) adenine and guanine and (b) thymine and cytosine systems.

$$R(t) = a_0 + a_1 e^{-\lambda_{2(1)}t} + a_2 e^{-\lambda_{2(2)}t} \quad (8)$$

Results of the fit to experimental spectra using the model given by eq 8, and listed in Table 3, produced two fractions with quite different relaxation constant values: one major fraction (a_1 > 65%) with λ_2 values in the range from ~7 to 13 MHz and another fraction with higher λ_2 values and smaller abundance. This latter fraction might represent the ^{111}In–molecule complex in a transient state after the decay of ^{111}In into ^{111}Cd when the electric quadrupole interaction rapidly changes because of the chemical rearrangement of the complex.

The rotational correlation time (τ_C) for each molecule was calculated for the observed major fraction [characterized by $\lambda_{2(1)}$ values in Table 3], with values of ν_Q and η taken from Table 1. An extremely slight damping of anisotropy was observed in the results of PAC measurements at 295 K for an aqueous solution of carrier free ^{111}In (^{111}Cd) due to a dynamic interaction characterized by a relaxation constant of 0.15 × 10^6

dx.doi.org/10.1021/bi401680h | Biochemistry 2014, 53, 3446−3456

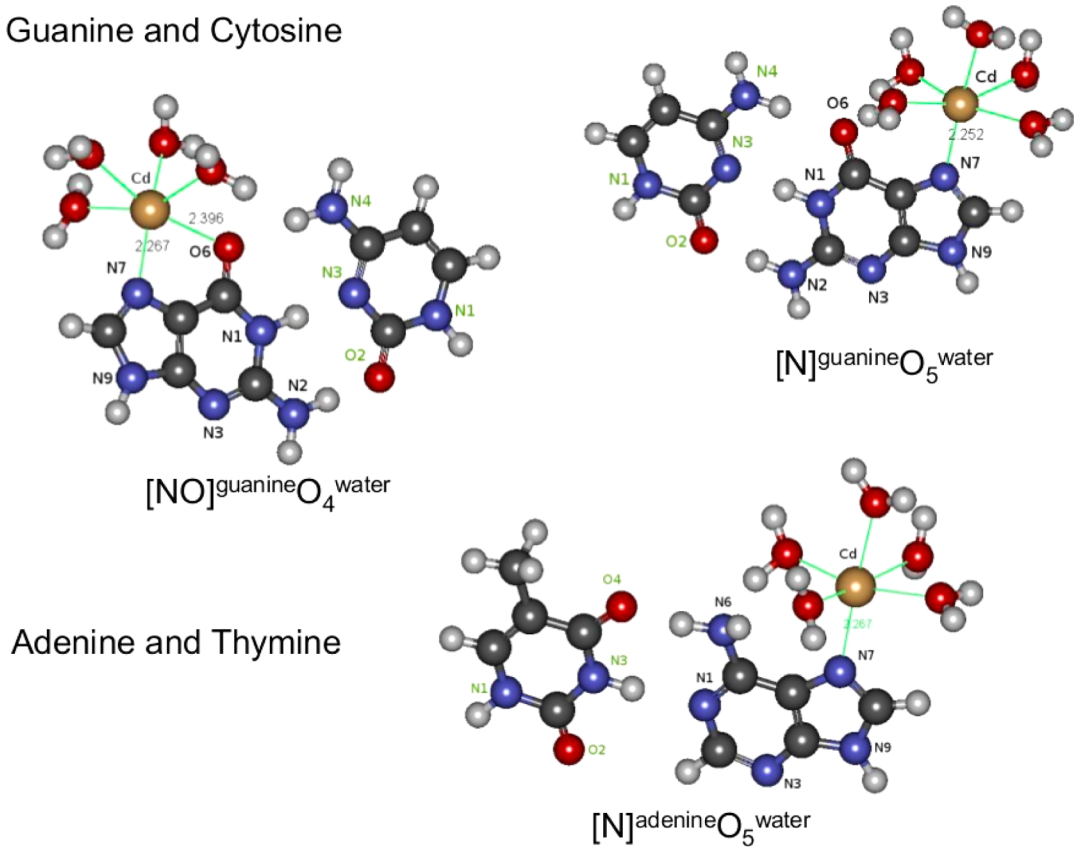

Figure 7. Geometry optimizations and Cd coordination for base pair systems studied herein.

s^{-1}, which corresponds to a ^{111}In (^{111}Cd)−hydroxyl complex at pH ∼3.0.[35]

The rotational correlation time describes the mobility of the molecule in a solution and can be estimated by the Stokes−Einstein relation:[36] $\tau_C = 4\pi a^3\xi/(3k_BT) = V\xi/(k_BT)$, where k_B is Boltzmann's constant and depends on the viscosity (ξ), temperature (T), and volume of the molecule ($V = 4\pi a^3/3$), which is considered a sphere of radius a. As all measurements were taken at the same temperature, and the viscosity of the solution was not expected to appreciably change once all samples had been prepared in aqueous solution, the value of τ_C was, therefore, directly proportional to the volume of the molecules. Values of τ_C for NB molecules vary from 13.3 × 10^{-11} s for adenine to 15.9 × 10^{-11} s for guanine, which are all within a relative narrow range, as expected. Results of τ_C for DNA molecules of A/J, C57BL/6, and B6AF1 strains, the original parents and the crossed offspring, are on the same order of magnitude with values in the range from ∼24 × 10^{-11} to ∼29 × 10^{-11} s, which are, however, quite different from the values for the DNA of the 20th generation of brother−sister inbreeding, ∼10 × 10^{-11} and 13 × 10^{-11} s for BXA1 and BXA2, respectively. According to the Stokes−Einstein equation, these results suggest that there is a considerable difference in the volume of DNA molecules for these two sets of molecules. However, according to τ_C values listed in Table 3, the volume of BXA1 and BXA2 molecules would be similar to the values of the nucleobases, which is unrealistic. Therefore, the model expressed by such an equation, which considers the molecule as a sphere, does not properly describe the rotational correlation time observed for DNA molecules. Consequently, other effects must be taken into account such as the shape of the molecule, important for long molecules, and the coordination of the Cd probe in the molecules (see the next subsection).

Geometry and EFG Calculations of the Cd−NB Complexes. *Ab initio* calculations were used to investigate the possible structures of the Cd−NB systems to correlate these structures with the EFG values at each Cd ion site. Tetrahedral, trigonal bypiramidal, and octahedral Cd coordination were considered as initial structures for the geometry relaxation. Because most of the measurements were performed in aqueous solutions of NBs, all models were simulated including water molecules to complete the first coordination sphere of the Cd ion. In Table 4, the notation used was BA^{water}, where B is the coordinating atom of the NB molecule and A^{water} is the oxygen atom of the water molecule that is coordinated to Cd ions. Figures 6 and 7 show the geometry optimization for the isolated NB and for base pair systems, respectively. These situations are described in Table 4.

In the case of the Cd−adenine complex, two optimized geometries were obtained: one with a distorted trigonal bypiramidal conformation (pentacoordination, $N_2O_3^{water}$) and another with a distorted octahedral conformation (hexacoordination, NO_5^{water}). In both configurations, the Cd ion was inserted by binding at N7. The Cd ion can also be coordinated at N6 of adenine, only in the $N_2O_3^{water}$ configuration (Figure 6a).

Similarly, three different final optimized geometries were obtained for the Cd−guanine complex. The Cd ion is bound only at N7 of guanine in NO_3^{water} and NO_5^{water} coordination with distorted tetrahedral and distorted octahedral coordination, respectively. On the other hand, in the $[NO]O_4^{water}$ configuration, the Cd ion is bound at N7 and also O6 of

dx.doi.org/10.1021/bi401680h | *Biochemistry* 2014, 53, 3446−3456

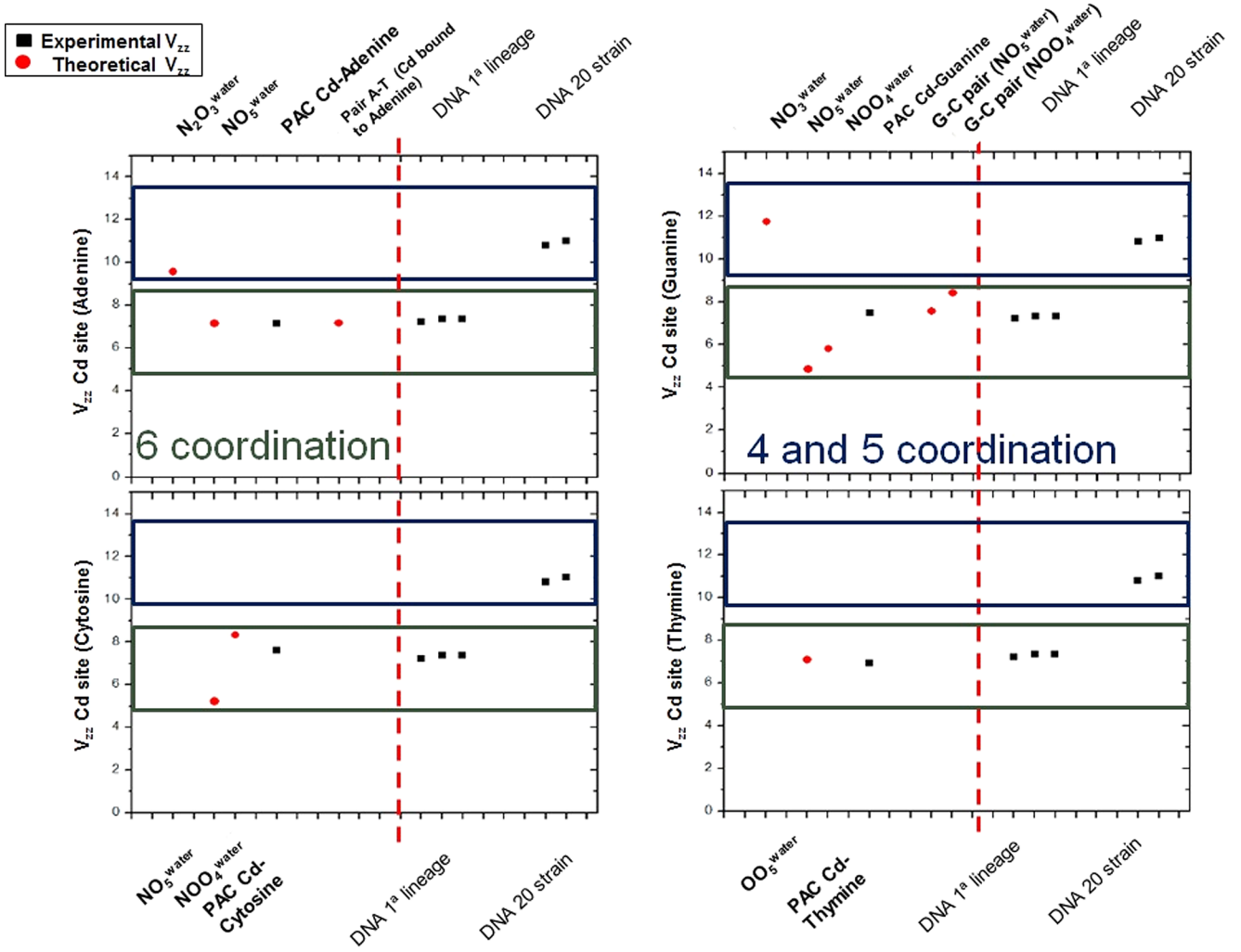

Figure 8. Summary of experimental and theoretical results. The red circles are the theoretical results and the black squares PAC measurements. The blue rectangles denote Cd tetra- and pentacoordination. The green rectangles denote hexacoordination.

guanine. The structure obtained for the Cd−thymine complex included the Cd ion bound to O4 of thymine, in an octahedral distorted coordination (Figure 6b). Finally, the fourth NB studied was the Cd−cytosine complex. Figure 6b shows two possible geometries for the Cd−cytosine species (NO_5^{water} and $[NO]O_4^{water}$). In the $[NO]O_4^{water}$ complex, the Cd ion is coordinated at N3 and O2 of cytosine, and in the NO_5^{water} complex, the Cd ion is coordinated at N3 of the cytosine. Apart from the isolated Cd−NB models studied, the Cd ion bound to the base pairs of cytosine and guanine (C-G) and adenine and thymine (A-T) was also investigated. The Cd ion coordination sphere was only simulated in the C-G and A-T base pair sites of the major groove region, with explicit coordinated water molecules. To provide meaningful structures, two observations were considered in these configurations: the steric hindrance due to the hydrogen atoms from methyl and amino groups and the intermolecular hydrogen bonding that restrains the interaction of the Cd ion with metal binding sites. The two most likely configurations for the Cd ion and G-C base pairs were then analyzed. In both configurations, the Cd ion is coordinated to N7 of guanine, as shown in Figure 7. In the case of the $[NO]^{guanine}O_4^{water}$ geometry (Figure 7a), the Cd ion is also coordinated to O6 of guanine. Only one configuration was obtained for the Cd ion at A-T pairs (Figure 7b), in which Cd ion has six coordination sites and is bound to N7 of adenine.

Table 4 shows the corresponding V_{zz} values for each NB and base pairs. The calculated V_{zz} values for all NBs are in the same range, corroborating the data observed in PAC measurements at 77 K (see Table 1). As expected, Cd ions with an octahedral coordination environment show V_{zz} values (range of 7.0−8.0 × 10^{21} V/m^2) are in better agreement with PAC measurements for DNA and NBs, as shown in Tables 1 and 4. Moreover, the V_{zz} values obtained from calculations with base pairs (Table 4) remained on the same order of magnitude as the V_{zz} values observed for the single NB molecules.

In Figure 8, we show a compilation of both PAC and DFT calculation results, according to the Cd coordination. An interesting point observed from the comparison between experimental V_{zz} values of different strains of mice infected with *T. cruzi* and DFT calculations for NBs is that V_{zz} values for DNA molecules of A/J, C57BL/6, and B6AF1 strains, which are the original parents and the crossed offspring, respectively, are consistent with Cd hexacoordination, as shown in Figure 8. On the other hand, DNA molecules of the 20th generation of brother−sister inbreeding (BXA1 and BXA2) showed V_{zz} values in good agreement with those of the systems that have Cd with tetra- or pentacoordination. Therefore, the observed

dx.doi.org/10.1021/bi401680h | *Biochemistry* 2014, 53, 3446−3456

difference in the dynamic behavior of the DNA molecules can be correlated to the V_{zz} values.

CONCLUSIONS

Values of V_{zz} obtained from measurements with both ^{111}In (^{111}Cd) and ^{111m}Cd (^{111}Cd) probe nuclei in NBs are in good agreement with the theoretical data provided by CP-PAW calculations proposed here. Comparison of experimental PAC results for NBs in aqueous solution with those for probe nuclei in water as well as comparison with DFT calculations in NBs indicates that the Cd ion is bound to NBs and DNA molecules and the coordination environment around the probes is almost the same for all NBs. Although the parent nuclei of ^{111}In (^{111}Cd) and ^{111m}Cd (^{111}Cd) are different, comparison of experimental data with DFT calculations also showed that both probes exhibit the same environment for all NBs. This may be explained by the fact that although ^{111}In and ^{111m}Cd could be bound to different sites of NB molecules, after the decay of ^{111}In by electron capture, a very fast rearrangement in the ^{111}In (^{111}Cd)−NB complex occurs, and therefore, the ^{111}Cd nuclei show the same environment as the ^{111m}Cd (^{111}Cd) probe nuclei. Measured values of V_{zz} for each NB are practically the same, and consequently, they do not indicate the exact location of the Cd ion when it is bound to DNA. However, some important conclusions can be reached on the basis of observations that emerge from the PAC measurement results. First, by DFT calculations in different environments, it was verified that experimental values of V_{zz} for DNA molecules of A/J, C57BL/6, and B6AF1 strains infected with *T. cruzi* (the original parents and the crossed offspring, respectively) are in good agreement with calculated results considering Cd ions hexacoordinated by the bases. Second, experimental values of V_{zz} for the DNA of the 20th generation of brother−sister inbreeding (BXA1 and BXA2) agree with calculations considering tetra- or pentacoordination geometry around the Cd ions. Moreover, results of dynamic interactions indicated that molecules for these two groups of DNA (original parents and first generation, and 20th generation) have quite different dynamic behavior. These observations provide an indication that a significant change in the local DNA structure occurs, considering these two groups of mice infected with *T. cruzi*. These results also open up the possibility of using PAC and *ab initio* calculations of hyperfine parameters as important tools in the characterization of these complicated biological scenarios.

AUTHOR INFORMATION

Corresponding Author

*E-mail: hmpetril@if.usp.br. Phone: 55 11 30916815.

Funding

We thank the Brazilian agencies FAPESP, CAPES, and CNPq for funding.

Notes

The authors declare no competing financial interest.

ACKNOWLEDGMENTS

We thank LCCA/CCE-USP and CENAPAD-SP for computational facilities.

REFERENCES

(1) Suits, B. H. (2006) in *Nuclear Quadrupole Resonance Spectroscopy* (Vij, D. R., Ed.) pp 65−96. Springer, New York.

(2) Christiansen, J. (1983) Hyperfine Interactions of Radioactive Nuclei. In *Current Topics in Physics* (Christiansen, J., Ed.) Springer, Berlin.

(3) Hemmingsen, L., Stachura, M., Thulstrup, P. W., Christensen, N. J., and Johnston, K. (2010) Selected applications of perturbed angular correlation of γ-rays (PAC) spectroscopy in biochemistry. *Hyperfine Interact. 197*, 255−267.

(4) Hemmingsen, L., and Butz, T. (2011) Perturbed Angular Correlations of γ-rays (PAC) Spectroscopy. In *Encyclopedia of Inorganic and Bioinorganic Chemistry*, pp 1−15, John Wiley and Sons, New York.

(5) Brisse, S., Barnabé, C., and Tibayrenc, M. (2000) Identification of six *Trypanosoma cruzi* phylogenetic lineages by random amplified polymorphic DNA and multilocus enzyme electrophoresis. *Int. J. Parasitol. 30*, 35−44.

(6) Roellig, D. M., Brown, E. L., Barnabé, C., Tibayrenc, M., Steurer, F. J., and Yabsley, M. J. (2008) Molecular typing of *Trypanosoma cruzi* isolates, United States. *Emerging Infect. Dis. 14*, 1123−1125.

(7) Roellig, D. M., Savage, M. Y., Fujita, A. W., Barnabé, C., Tibayrenc, M., Steurer, F. J., and Yabsley, M. J. (2013) Genetic variation and exchange in *Trypanosoma cruzi* isolates from the United States. *PLoS One 8*, e56198.

(8) Sletten, E. (2009) in *Metal Complex−DNA Interactions* (Hadjiliadis, N., and Sletten, E., Eds.) John Wiley & Sons, Ltd., Chichester, U.K.

(9) Manning, G. S. (2009) The molecular theory of polyelectrolyte solutions with applications to the electrostatic properties of polynucleotides. *Q. Rev. Biophys. 11*, 179−246.

(10) Yamane, T., and Davidson, N. (1961) On the Complexing of Desoxyribonucleic Acid (DNA) by Mercury Ion. *J. Am. Chem. Soc. 83*, 2599−2607.

(11) Sletten, E. (1994) Interaction of Mercury(II) with the DNA Dodecamer CGCGAATTCGCG. A ^{1}H and ^{15}N NMR Study. *J. Am. Chem. Soc. 116*, 3240−3250.

(12) Sigel, R. K. O., and Sigel, H. (2010) A stability concept for metal ion coordination to single-stranded nucleic acids and affinities of individual sites. *Acc. Chem. Res. 43*, 974−984.

(13) Da Costa, C. P., and Sigel, H. (2003) Acid-base and metal ion binding properties of guanylyl(3′→5′)guanosine (GpG-) and 2′-deoxyguanylyl(3′→5′)-2′-deoxyguanosine [d(GpG)-] in aqueous solution. *Inorg. Chem. 42*, 3475−3482.

(14) Knobloch, B., Sigel, H., Okruszek, A., and Sigel, R. K. O. (2007) Metal-ion-coordinating properties of the dinucleotide 2′-deoxyguanylyl(5′→3′)-2′-deoxy-5′-guanylate (d(pGpG)3-): Isomeric equilibria including macrochelated complexes relevant for nucleic acids. *Chemistry 13*, 1804−1814.

(15) Blöchl, P. (1994) Projector augmented-wave method. *Phys. Rev. B: Condens. Matter Mater. Phys. 50*, 17953−17979.

(16) Car, R. (1985) Unified Approach for Molecular Dynamics and Density-Functional Theory. *Phys. Rev. Lett. 55*, 2471−2474.

(17) Kohn, W., and Sham, L. J. (1965) Self-Consistent Equations Including Exchange and Correlation Effects. *Phys. Rev. 140*, A1133−A1138.

(18) Perdew, J. P., Burke, K., and Ernzerhof, M. (1996) Generalized Gradient Approximation Made Simple. *Phys. Rev. Lett. 77*, 3865−3868.

(19) Margl, P., Schwarz, K., and Blöchl, P. E. (1993) First-Principles Calculations of Organometallic Compounds. In *Computationals for the Nano-Scale* (Blöchl, P. E., Joachim, C., and Fisher, A. J., Eds.) pp 153−162, Springer, Dordrecht, The Netherlands.

(20) Wu, G., Dong, S., Ida, R., and Reen, N. (2002) A solid-state ^{17}O nuclear magnetic resonance study of nucleic acid bases. *J. Am. Chem. Soc. 124*, 1768−1777.

(21) Mahato, D. N., Dubey, A., Pink, R. H., Scheicher, R. H., Badu, S. R., Nagamine, K., Torikai, E., Saha, H. P., Chow, L., Huang, M. B., and Das, T. P. (2008) Theoretical investigation of nuclear quadrupole interactions in DNA at first-principles level. *Hyperfine Interact. 181*, 81−86.

(22) Hossain, Z., and Huq, F. (2002) Studies on the interaction between Cd^{2+} ions and nucleobases and nucleotides. *J. Inorg. Biochem. 90*, 97−105.
(23) Ochoa, P. A., Rodríguez-Tapiador, M. I., Alexandre, S. S., Pastor, C., and Zamora, F. (2005) Structural models for the interaction of Cd(II) with DNA: trans-$[Cd(9\text{-RGH-N7})_2(H_2O)_4]^{2+}$. *J. Inorg. Biochem. 99*, 1540−1547.
(24) Pye, C. C., Tomney, M. R., and Rudolph, W. W. (2006) Cadmium hydration: Hexacoordinate or heptacoordinate? *Can. J. Anal. Sci. Spectrosc. 51*, 140−146.
(25) Petrilli, H. M., Blöchl, P., Blaha, P., and Schwarz, K. (1998) Electric-field-gradient calculations using the projector augmented wave method. *Phys. Rev. B 57*, 14690−14697.
(26) Marshall, J. D., Mu, J. L., Cheah, Y. C., Nesbitt, M. N., Frankel, W. N., and Paigen, B. (1992) The AXB and BXA set of recombinant inbred mouse strains. *Mamm. Genome 3*, 669−680.
(27) Trischmann, T., Tanowitz, H., Wittner, M., and Bloom, B. (1978) *Trypanosoma cruzi*: Role of the immune response in the natural resistance of inbred strains of mice. *Exp. Parasitol. 45*, 160−168.
(28) Shpinkova, L. G., Carbonari, A. W., Nikitin, S. M., and Mestnik-filho, J. (2002) Influence of electron capture after-effects on the stability of ^{111}In (^{111}Cd)-complexes with organic ligands. *Chem. Phys. 279*, 255−263.
(29) Butz, T. (1989) Analytic Perturbation Functions for Static Interactions in Perturbed Angular Correlations of γ- rays. *Hyperfine Interact.*, 189−228.
(30) Karlsson, E., Mathias, E., and Siegbahn, K. (1964) *Perturbed Angular Correlation*, North-Holland Publishing Co., Amsterdam.
(31) Herzog, P., Freitag, K., Reuschenbach, M., and Walitzki, H. (1980) Nuclear orientation of ^{111m}Cd in Zn and Be and the quadrupole moment of the 245 keV state. *Z. Phys. A: At. Nucl. (1975) 294*, 13−15.
(32) Dogra, R., Junqueira, A. C., Saxena, R. N., Carbonari, A. W., Mestnik-Filho, J., and Moralles, M. (2001) Hyperfine interaction measurements in $LaCrO_3$ and $LaFeO_3$ perovskites using perturbed angular correlation spectroscopy. *Phys. Rev. B 63*, 2241041−2241049.
(33) Abragam, A., and Pound, R. V. (1953) Influence of Electric and Magnetic Fields on Angular Correlations. *Phys. Rev. 92*, 943−962.
(34) Errico, L., Rentería, M., and Petrilli, H. M. (2007) Cd in SnO: Probing structural effects on the electronic structure of doped oxide semiconductors through the electric field gradient at the Cd nucleus. *Phys. Rev. B 75*, 1552091−1552099.
(35) Demille, G. R., Livesey, D. L., Mailer, K., and Turner, S. R. (1976) Perturbed γ-Ray Directional Correlation Studies of Indium-(III) complexing in Aqueous Solution. *Chem. Phys. Lett. 44*, 164−168.
(36) Bauer, R., Limkilde, P., and Johansen, J. T. (1976) Low and high pH form of cadmium carbonic anhydrase determined by nuclear quadrupole interaction. *Biochemistry 15*, 334−342.